7-7 Terahertz Remote-Sensing of the Venusian Atmosphere: Observations Using the Nobeyama Millimeter Array

SAGAWA Hideo

Venusian spectra at the terahertz region are characteristic of several rotational absorption lines of minor constituents superposed on a continuum of the atmospheric thermal emission. The intensity of the continuum emission varies from 700 to 200 K with increasing the observing frequency from radio to terahertz region, which enables us to observe the Venusian atmosphere in a wide vertical range: from the surface to the cloud top. The rotational lines provide us effective tools not just to retrieve the vertical and horizontal distribution of minor constituents but also to measure the wind velocity via Doppler-shift of the line center frequency. In this paper, the results of the aperture synthesis observations of Venus using the Nobeyama Millimeter Array are presented.

Keywords
Terahertz radiation, Venus, Remote sensing, Interferometer, Aperture synthesis

1 Introduction

Venus has a CO_2 atmosphere with a surface pressure reaching 90 bar. Clouds made of sulfuric acid droplets cover the entire globe to a thickness of several kilometers near an altitude of 50 km. The large amount of CO_2 gas yields the so-called "greenhouse effect"; the atmospheric temperature on the surface of Venus is higher than 700 K. In addition to these unique features in the atmospheric structure, the atmospheric dynamic in the lower atmosphere of Venus (from the surface to an altitude of approximately 70 km) is characterized by a fast, continuous, westward circulation (known as a "super rotation"), one that moves 60 times faster than the rotation rate of the planet. Why does the atmospheric environment of Venus differ so markedly from that of Earth? The key to this question lies in a clarification of the present climate system of Venus.

For observational study of the Venusian climate system, a three-dimensional understanding of its atmospheric structure and circulations is indispensable. To this end, it is important that we be able to observe through the thick Venusian atmosphere, to target various altitudes. However, the opaque atmosphere with clouds restricts attempts at observation below the cloud top (at an altitude of around 70 km) using the visible wavelengths. In the 1980s, "atmospheric windows" where the CO_2 atmosphere becomes optically thin were discovered in the near-infrared region. These windows enable us to observe the atmosphere below the cloud layer on the night side of Venus[1]. However, even using such windows, limitations remain: we can only obtain information on a limited range of altitudes in the lower atmosphere, and we can observe only the night side of the planet.

Using remote sensing in the terahertz region can help break through these limitations. At lower frequency ranges like 0.1 THz, the Venusian atmosphere is more transparent than at the visible wavelengths, and the scattering and absorption effects of the clouds are sometimes negligible. In addition, Venus is much brighter than the Sun in the terahertz region. Thus, using terahertz wavelengths enables, for the first time, observation below the clouds on both the day and night sides of Venus. Terahertz observations have another useful characteristic: thanks to the heterodyne spectroscopic techniques, a very high dispersion spectroscopy can be achieved in the terahertz region. The high dispersion spectroscopy enables us to view the rotational transition lines of even minor constituents (such as CO and H_2O) in the mesosphere (from 70 to 100 km in altitude). It is possible to retrieve the vertical distribution of these minor constituents and the vertical profile of the atmospheric temperature as well as to observe the Doppler shift of the center frequency of the absorption/emission line caused by Venusian atmospheric circulation.

This article discusses the effectiveness of terahertz remote sensing of the Venusian atmosphere, mainly focusing on the results of observations of Venus in the 0.1-THz range conducted with the Nobeyama Millimeter Array. First, Section **2** briefly describes the aperture synthesis observation of Venus. Section **3** and later sections describe the results of observations of the Venusian atmosphere near altitudes of 50 km and 100 km derived by analyzing the continuum radiation and absorption line of ^{12}CO, respectively.

2 Aperture synthesis imaging using an interferometer

A radio interferometer is an observational instrument that correlates signals received by two or more telescopes (referred to as antenna elements) placed at separate positions; the interferometer then combines the signals to synthesize an image (i.e., aperture synthesis) as if taken by a single large-aperture telescope. The minimization of the elongation that can be resolved by a telescope has a theoretical lower limit, known as the "diffraction limit," which is proportional to the size of the main reflector (i.e., antenna parabola) of the telescope and the shortness of the observation wavelength. Optical observation using recent ground based telescopes generally offers spatial resolution of 1" or higher. When we attempt to implement a comparable spatial resolution in the terahertz region, for instance at 0.1 THz, we require an unrealistically immense parabola with a 750-m aperture. Aperture synthesis imaging using interferometers was devised to solve this problem. The Nobeyama Millimeter Array consists of six 10-m antenna elements separated by intervals of up to 350 m. In observation at 0.1 THz, the array provides a spatial resolution as high as approximately 2". Such a spatial resolution in the terahertz region is among the best in the world, comparable even to the CARMA interferometer in the U.S. and Europe's Plateau de Bure interferometer.

This section does not describe the details of the data analysis but rather comments on the important points to consider when using an interferometer in planetary observations. The details of the signal processing — from the signal obtained in each antenna element to interferometer output—and the method of image synthesis are found in Thompson et al. (2001)[2].

2.1 Resolving out of an extended object with uniform brightness distribution

Although interferometers offer high spatial resolution, one of the weaknesses of these devices is their lack of sensitivity to radio sources featuring a uniform spatial-distribution structure. The data, $o(u, v)$ (referred to as visibility), obtained by the interferometer corresponds to the Fourier transformation of the brightness distribution, $I(x, y)$, of the observed object:

$$o(u,v)=\int_{-\infty}^{+\infty}\int_{-\infty}^{+\infty} I(x,y)e^{2\pi i(ux+vy)}dxdy \quad (1)$$

The angular dependency of the primary beam pattern is ignored in Equation (1). (u, v) indicate the spatial frequency components of (x, y) and are determined by the baseline length and observation frequency. As the baseline length is subject to a physical restriction (i.e., the elements cannot be placed closer than the antenna diameter), we cannot observe small spatial frequency components near $(u, v) = 0$. In other words, interferometers cannot observe brightness components having a structure more extended than a specific spatial scale.

This problem—referred to as "resolving out" or "missing flux"—becomes extremely serious when attempting to observe an object with an extended structure such as a planet. Figure 1 shows the initial synthesized image from simulated visibilities assuming a disk radio source with a uniform brightness in an apparent diameter of 10" to 40", observed by the C-array configuration (an array configuration with a baseline length of 26 m to 164 m) of the Nobeyama Millimeter Array. When the apparent diameter exceeds 20", the disk structure is not reproduced (the image is instead separated into two parts), and the observable flux intensity also decreases.

This problem is solved by assuming a model visibility for the missing components. As a first-order approximation, the brightness distribution of a planet can be assumed to correspond to a uniform disk with a limb-darkening effect, which formulation is found in Butler and Bastian (1999)[3]. By obtaining the model visibility of the disk brightness distribution that matches the measured visibilities, we can derive the total flux density for $(u, v) = 0$ (Fig. 2).

2.2 Deconvolution of side lobe pattern

The principle of image synthesis using the visibility measured by the interferometer is shown by the inverse Fourier transformation of Equation (1). However, in practical observation, we need to consider the discreteness and finite number of sampling points in the spatial frequency domain. By introducing the sampling function, $s(u, v)$, which takes a value of either 0 or 1, the measured visibility is expressed as $o_{obs}(u, v) = s(u, v)\ o(u, v)$. When this equation is inverse-Fourier-transformed, the inverse transformation, $S(x,y)$, of the sampling function is convoluted in the radio source structure, $I(x,y)$. $S(x,y)$ is referred to as the "synthesized beam" and features a side-lobe pattern with alternating positive and negative values outside the main beam. Due to the effects of this side-lobe pattern, the initial synthesized images in Fig. 1 appear to indicate radio sources with positive and negative flux-

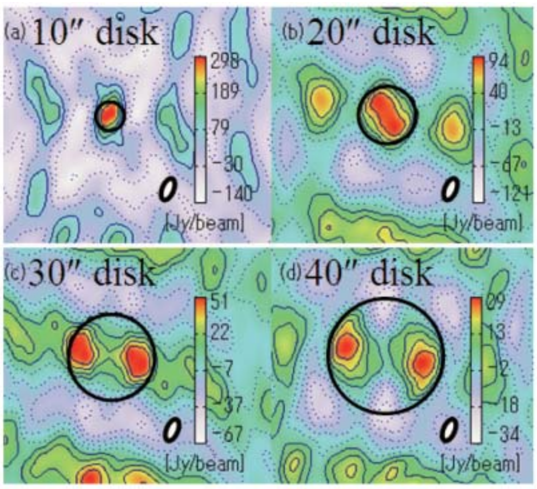

Fig. 1 *Simulation of the resolving out*

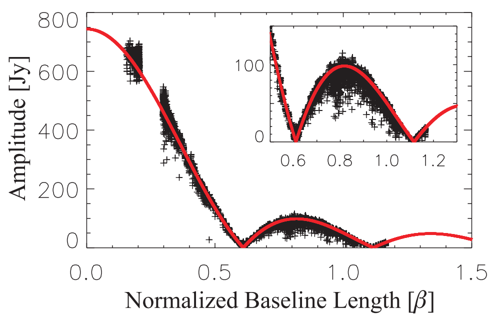

Fig. 2 *Measured visibilities of Venus (black dots) and best-fitted model visibilities (red curve) of limb-darkening disk*

The horizontal axis corresponds to the spatial frequency normalized by the Venusian apparent size. The total flux density (disk-averaged brightness temperature) for $(u, v) = 0$ obtained by fitting is 337 K.

es outside of the disk given by the model. We need to remove the side-lobe pattern of the synthesized beam from the initial synthesized image to obtain a real image.

For point-like radio sources, several side-lobe deconvolution techniques have been established[4]. However, extended radio sources such as a planet cannot be processed in the same way as a point-like source. This is because the false signal due to the side-lobe pattern overlaps with the extended radio source and may obscure the fine details of amplitude of the true brightness distribution. For example, the image on the left of Fig. 3 shows an initial synthesized image of Venus. Here we cannot identify the brightness distribution in fine structural detail. To solve this problem, we need to deconvolve the side lobe pattern using a method developed for extended radio sources[5]. We first subtract the extended uniform brightness component from the measured visibilities. The initial image (Fig. 3, middle) synthesized from the residual visibilities is treated as a collection of minute point-like radio sources. We then repeatedly apply side-lobe deconvolution for point-like radio sources to the residual image. Finally, we add the subtracted uniform brightness component to produce the real image of Venus in which the resolve out feature described in **2.1** is also corrected (Fig. 3, right).

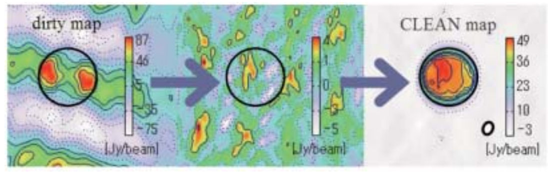

Fig.3 *Side-lobe deconvolution*

See the main text for details. The black circle indicates the position at which the Venus disk should be present. Although not discussed in the main text, we reduced the noise pattern of the image by applying the phase calibration technique[6] known as “self-calibration.”

2.3 Comments on observation at higher frequencies

The spatial frequency of measured visibilities is proportional to baseline length and observation frequency. If we perform observation using the same antenna array at two different wavelengths of 0.1 THz and 0.5 THz, we note that observation at 0.5 THz offers visibility at higher spatial frequency and higher spatial resolution in the synthesized image. On the other hand, with observation at 0.5 THz, the minimum spatial frequency is larger than that at 0.1 THz, and thus a larger amount of the flux resolves out. As shown in the visibility distribution illustrated in Fig. 2, at a spatial frequency larger than the first null (β: approximately 0.6) of visibility, the flux intensity of the planet rapidly decreases. As the spatial frequency increases, the noise generated by the fluctuation of the earth’s atmosphere significantly increases. Thus, it is difficult to fit the model visibilities of the limb-darkening disk to observed values that do not contain spatial frequency components smaller than the first null. In such cases, we need to conduct complementary observations with a single dish radio telescope to measure the total flux density itself at $(u, v) = 0$.

At a high observation frequency, the narrow field of view of the interferometer also poses a problem. The field of view of the interferometer is determined by the full width at half maximum (FWHM) of the primary beam pattern of each element. For the 10-m antenna of the Nobeyama Millimeter Array, the field of view is approximately 65" at 0.1 THz. When we assume that the aperture of the antenna is constant, the field of view decreases with an increase in observation frequency. Assuming that we perform observation with an interferometer composed of 10-m antennas at 0.5 THz, the field of view decreases to 15". In this case we can observe the entire image of Venus only near the superior conjunction, when the apparent diameter is small. In this case, mapping Venus near the inferior conjunction with a single dish antenna produces a larger effective spatial resolution.

3 Observing below clouds: Mapping a continuum emission

3.1 Significance of terahertz continuum observation

The optical thickness of the Venusian atmosphere in the terahertz region is mainly determined by the pressure induced continuum absorption of CO_2. This absorption is caused by the dipole moment excited within the CO_2 molecules due to the collision between the CO_2 molecules. Figure 4a shows the brightness temperature of Venus in the radio to terahertz ranges, calculated by solving the radiative transfer equation taking the CO_2 continuum absorption into consideration. From the vertical temperature profile of the Venusian atmosphere (Fig. 4b), we can find the source altitude of the observed thermal radiation. The intensity of the continuum absorption of CO_2 monotonically increases with an increase in frequency in the terahertz region[7]. As a result, we observe the brightness temperature change "continuously" from approximately 700 K to 200 K in the radio to terahertz ranges. This feature clearly demonstrates the effectiveness of continuum observation of the Venusian atmosphere in the radio to terahertz range. By setting the observation frequency appropriately, we can freely observe an arbitrary altitude from the surface to the cloud top.

3.2 Observation using the Nobeyama Millimeter Array

Figure 5 shows 0.1-THz (103-GHz) continuum maps of Venus observed with the Nobeyama Millimeter Array. The images show a fluctuation in the brightness temperature from 300 K to 380 K inside the Venus disk. This inhomogeneity was also pointed out in a past study[10]. Accordingly, we performed observation at a higher spatial resolution than that employed in the past study. As a result, we confirmed spatially finer brightness fluctuations, with larger amplitude values than those reported in the past study.

The brightness temperature, 300 K to 380 K, obtained in this observation corresponds to the temperature at altitudes around 50 km, which corresponds to the bottom of the cloud layer. The optical thickness of the cloud layer of Venus is considered extremely thin in

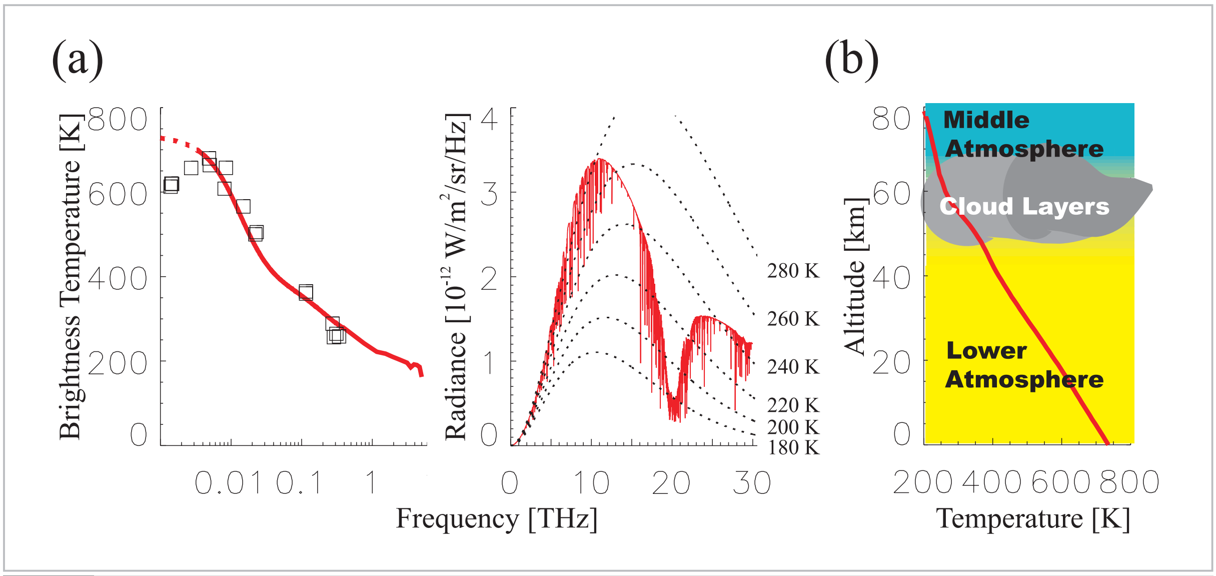

Fig.4 *(a) Calculated brightness temperature of Venus. The Planck functions at 180 K to 280 K are superposed. The boxes indicate values measured in past radio observations [8]. As this calculation does not take surface emissivity into consideration, it does not agree with the observation results in the range of centimeter wavelengths. (b) Standard vertical temperature structure of Venus [9]. While we can observe through to the surface using centimeter wavelengths, we can observe the atmosphere from the cloud bottom to the cloud top in the terahertz region.*

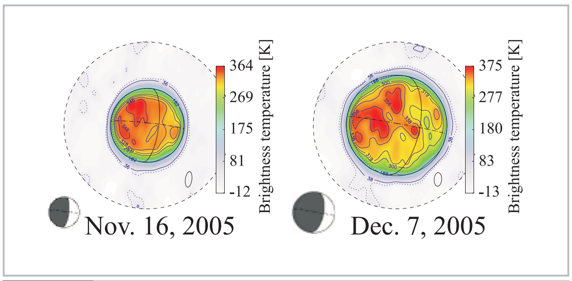

Fig.5 *103-GHz continuum map of Venus observed with the Nobeyama Millimeter Array*

The apparent diameter of Venus is 30" and 40" , respectively. The lower right ellipse indicates the FWHM size of the synthesized beam. The dotted circle outside of Venus indicates the field of view of the interferometer.

the 0.1-THz range and does not yield fluctuation in brightness temperature[11]. Apart from the spatial variation in cloud opacity, the inhomogeneity in brightness temperature may be caused by the spatial variations in the atmospheric temperature and the distribution of SO_2 and H_2SO_4 gases, which feature a cluster of rotational transition lines near the 0.1-THz range. The temperature fluctuation in the horizontal plane near an altitude of 50 km indicated in past in-situ observations (including those by the Pioneer Venus probes) is considered to be approximately 10 K[9]. The spatial variations in the SO_2 and H_2SO_4 distribution were observed by the Vega probes[12] and in the radio occultation experiments[13] of the Magellan spacecraft. However, when we evaluated the change in the brightness temperature caused by these inhomogeneities by solving the radiative transfer equations, we obtained a brightness temperature of only approximately 340 K to 360 K. If we try to explain our observed results, from 300 K to 380 K, based on the atmospheric temperature fluctuation and/or the SO_2 and H_2SO_4 distributions, we need to assume greater inhomogeneities than have been observed to date. At present, we lack sufficient data to draw a definite conclusion for such large inhomogeneities, and we cannot confirm the physical processes causing the brightness variations in the 0.1-THz continuum emissions. Nevertheless, we can say that the observed inhomogeneity of brightness temperatures provides new knowledge concerning the Venusian atmospheric state near an altitude of 50 km, which was previously discussed in the context of only the limited information on the cloud opacity distribution provided using near-infrared wavelengths.

3.3 Future of terahertz continuum observation

The possibility of observing a broadband continuum spectrum at a bandwidth of approximately 10 GHz is an exciting one. Using such a broad band spectrum will enable us to visualize the atmospheric structure from the altitude of 40 km to 60 km three-dimensionally. In addition, we will be able to use the difference in frequency dependencies of the absorption coefficients between SO_2 and H_2SO_4 to distinguish the effects of these two compounds.

When the observation frequency increases, the effects of absorption and scattering by cloud particles are also considered to increase. Increasing the number of high-frequency terahertz-wave observations will open the door to the determination of the three-dimensional distribution of the physical parameters of the clouds on both the day and night sides. However, we must first acquire the optical constants of the liquid sulfuric acid in the terahertz range in the laboratory.

4 Measurement of Venusian mesospheric dynamics

4.1 Observation of ^{12}CO (J = 1 – 0)

Using high-dispersion spectroscopy, we can observe the rotational transition lines of various minor atmospheric constituents. For Venus, atmospheric constituents such as ^{12}CO, ^{13}CO, H_2O, HDO, and SO_2 have been observed in the frequency range from 0.1 THz to 0.5 THz[14][15]. The weighting function at the frequencies near the center of these absorption lines has a peak in the mesosphere (near an altitude of 70 km to 100 km) of the Venusian atmosphere. Thus, while the observation using the continuum emission described in Section **3** provides information on the atmosphere below the clouds, observation using rotational lines provides information on the atmosphere above the clouds.

The author performed mapping observation of ^{12}CO (J= 1 – 0, 115.271 GHz) using the Nobeyama Millimeter Array. The frequency resolution of the spectral correlator used is 31.25 kHz (velocity resolution of 80 m/s). Figure 6 shows the spectra extracted from the data near noon and midnight on Venus (local time of 14:00 and 23:00). These spectra differ in (1) absorption depth and (2) line center frequency. From the difference in the absorption depth, we can determine that CO is more concentrated on the night side than on the day side near an altitude of 100 km. This observation agrees with the results of a past study[14]. The CO in the Venusian atmosphere is formed by photodissociation of CO_2 in the day side. The CO enrichment on the night side, where the CO source is not present, indicates that the atmospheric circulation that transports CO from the day side to the night side (Subsolar-Antisolar flow) takes place near an altitude of 100 km.

The Doppler shift—such as that generated by the component in the direction of the radial velocity of the wind, as shown in (2) above—provides a direct visualization of the Subsolar-Antisolar flow. Figure 7 maps the amount of Doppler shift (frequency difference from the center-line frequency of the sub-observation point) on different days. In data from April 2004 and November 2005, the day side of Venus shows blue shifts, and the night side shows red shifts. Such a pattern of Doppler shift direction on the day and night sides suggests the wind is blowing from the day side toward the night side. This pattern is similar to the pattern created by the super rotation-like flow (i.e., the westward zonal flow). However, the results from April 2006, when the day and night positions are reversed, shows that Subsolar-Antisolar flow is more dominant than the westward zonal flow. The result from December 2005 shows that the local wind does not always flow from the day side to the night side. These results indicate intense variability in the mesospheric atmospheric circulation.

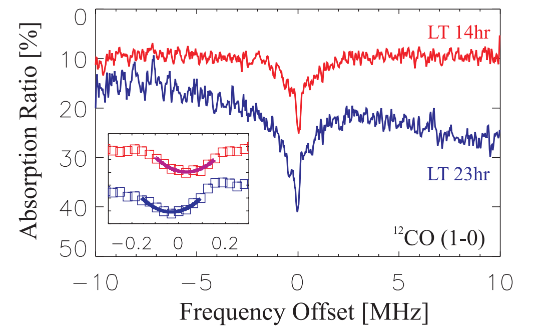

Fig.6 ^{12}CO spectra extracted at different local time on Venus

The horizontal axis is the frequency difference from the rest frequency. The enlarged image of the range near the absorption center shows the difference in the extent of the Doppler shift.

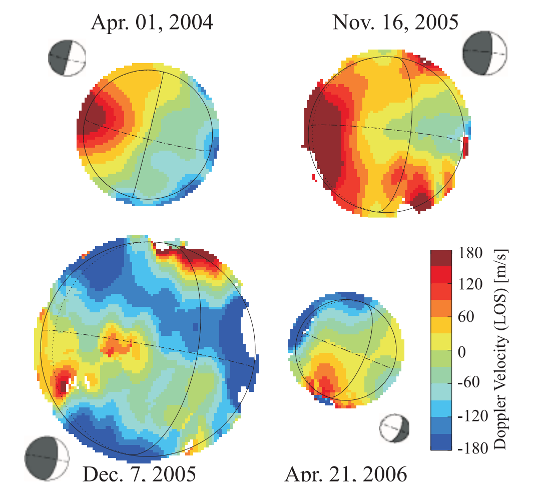

Fig.7 Doppler-shift distribution. The direction going away from the earth is defined as the positive direction (red shift).

4.2 Future terahertz absorption line observation

How is the wind velocity distributed between the Subsolar-Antisolar flow near an altitude of 100 km and the super rotation dominating the motion of the lower atmosphere? This is a particularly important question when discussing the mechanism of formation of super rotation. In addition to the ^{12}CO observed in this study, rotational lines of multiple minor constituents of the Venusian mesosphere are also present in the terahertz range. By observing two or more of these rotational lines with different optical thickness, we can observationally clarify the vertical distribution of wind velocity in the mesosphere. For example, Fig. 8 shows the weighting functions for the observations of different orders of CO isotopes rotational lines. The figure shows that the combination of these observations can provide information on the atmosphere at altitudes from 80 km to 100 km. Simultaneously observing CO isotopes with different optical thicknesses is also a meaningful means of increasing the precision of retrieval of the vertical distributions of molecular mixing ratio and temperature.

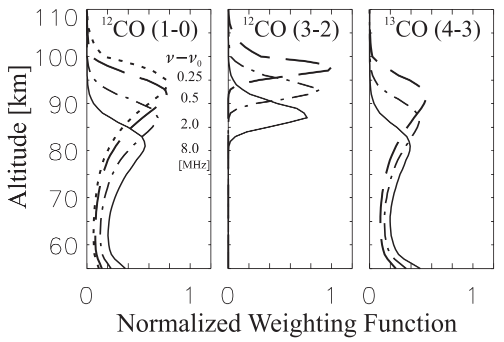

Fig.8 Weighting functions expected when CO isotopes with different rotational transitions are observed

5 Conclusions

This article discusses the effectiveness of remote sensing using terahertz waves in the context of research into the Venusian atmosphere. Specifically, aperture synthesis imaging using an interferometer allows for observations providing spatial resolution of the planet (Section **2**). The thermal radiation observed by terahertz waves provides the one available method for remote sensing at an arbitrary altitude, from the bottom of the cloud layer to the cloud top in the Venusian atmosphere, in the day and night (Section **3**). The molecular rotational transition lines present in the terahertz range are most suitable for observing atmospheric circulation in the Venusian mesosphere, for which only limited visualization techniques were previously available (Section **4**).

Acknowledgements

This article is based on the author's own graduate thesis. Many people provided help and advice, including Professor Masato Nakamura, Associate Professor Yoshimi Kitamura (JAXA), Dr. George L. Hashimoto (Kobe University), and Dr. Koichiro Nakanishi (National Astronomical Observatory of Japan) in the observations using the Nobeyama Millimeter Array, in addition to discussions of the data analyses. The operational staff of the Nobeyama Millimeter Array also provided substantial support to the observations. I would like to take this opportunity to express my sincere gratitude to all of the foregoing individuals.

References

1 Carlson, R. W., et al., "Variations in Venus cloud particle properties: A new view of Venus's cloud morphology as observed by Galileo Near-Infrared Mapping Spectrometer", Planet. Space Sci., 41, 477-485, 1993.

2 Thompson, A. R., J. M. Moran, and G. W. SwensonJr., "Interferometry and synthesis in radio astronomy", Second edition, Germany, Wiley-VCH, 2001.

3 Butler, B. J., and T. S. Bastian, "Solar system objects", in Synthesis imaging in radio astronomy Ⅱ, eds. G. B. Taylor, C. L. Carilli and R. A. Perley, San Francisco, Astronomical Society of the Pacific, 625-656, 1999.

4 Cornwell, T. J., “The application of closure phase to astronomical imaging”, Science, 245, 263-269, 1989.

5 de Pater, I., “Radio images of the planets”, Annu. Rev. Astron. Astrophysics, 28, 347-399, 1990.

6 Cornwell, T., and R. Braun, “Deconvolution”, in Synthesis imaging in radio astronomy, eds. A. P. Richard, F. R. Schwab and A. H. Bridle, San Francisco, the Astronomical Society of the Pacific, 109-121, 1989.

7 Gruszka, M., and A. Borysow, “Roto-translational collision-induced absorption of CO_2 for the atmosphere of Venus at frequencies from 0 to 250cm^{-1}, at temperatures from 200 to 800K”, Icarus, 129, 172-177, 1997.

8 Butler, B. J., et al., “Accurate and Consistent Microwave Observations of Venus and Their Implications”, Icarus, 154, 226-238, 2001.

9 Seiff, A., et al., “Models of the structure of the atmosphere of Venus from the surface to 100 kilometers altitude”, Adv. Sp. Res., 5, 3-58, 1985.

10 de Pater, I., F. P. Schloerb, and A. Rudolph, “Venus imaged with the Hat Creek interferometer in the J = 1−0 CO line”, Icarus, 90, 282-298, 1991.

11 Fahd, A. K., and P. G. Steffes, “Laboratory measurement of the millimeter wave properties of liquid sulfuric acid”, J. Geophys. Res., 96, 17471-17476, 1991.

12 Bertaux, J. L., et al., “VEGA 1 and VEGA 2 entry probes: An investigation of local UV absorption (220-400 nm) in the atmosphere of Venus (SO_2, aerosols, cloud structure)”, J. Geophys. Res., 101, 12709-12746, 1996.

13 Kolodner, M. A., and P. G. Steffes, “The microwave absorption and abundance of sulfuric acid vapor in the Venus atmosphere based on new laboratory measurements”, Icarus, 132, 151-169, 1998.

14 Lellouch,E., et al., “Global circulation, thermal structure, and carbon monoxide distribution in Venus’ mesosphere in 1991”, Icarus, 110, 315-339, 1994.

15 Gurwell, M. A., et al., “SWAS observations of water vapor in the Venus mesosphere”, Icarus, 188, 288-304, 2007.

***SAGAWA Hideo**, Ph.D.*

Max Planck Institute for Solar System Research, Germany

Remote Sensing of the Planetary Atmosphere